

## **Structural, morphological and optical characterization of as-deposited and annealed quaternary $\text{Se}_{50}\text{Cd}_{20}\text{Cu}_{20}\text{Te}_{10}$ chalcogenide thin film**

**Pramesh Chandra\*, Arvind Kumar Verma, R. K. Shukla and Anchal Srivastava**

*Department of Physics, University of Lucknow, Lucknow – 226007, India.*

### **Abstract**

In the present study, the effects of annealing on structural, morphological and optical properties of metal added quaternary chalcogenide thin film  $\text{Se}_{50}\text{Cd}_{20}\text{Cu}_{20}\text{Te}_{10}$  have been reported. The film is deposited on glass substrate by thermal evaporation technique. The bulk sample used for depositing the film is synthesized using melt quenching method. Post deposition, the film is annealed at  $125^{\circ}\text{C}$  ( $398\text{K}$ ) for two hours. Structural studies show that annealing introduces polycrystalline structure in amorphous phases of the as-deposited film whereas morphological images show densification and enlargement of relatively scattered nano sized grains of the as-deposited film. Absorption spectra show higher absorption for the annealed film in the near infrared range whereas optical transmission spectra show negligible transmission in the ultraviolet and visible regions and reduction of transmission in the near infrared range. Photoluminescence spectra studied at three different excitation wavelengths – 330 nm, 380 nm and 430 nm – show green emission with markedly higher intensities for the annealed film in all the three cases.

**Keywords:** Chalcogenide, Melt quenching, Annealing, Near infrared, Photoluminescence.

### **1. INTRODUCTION**

Applications of chalcogenides in thin film form in various fields such as electronics, optoelectronics, nanotechnology industry etc. have been reported in the literature.

Interest in the chalcogenides of metals, semiconductors and transition metals has increased because of their tunable properties which make them useful in various devices [1-5]. Techniques used for the preparation of chalcogenide thin films give advantages of convenience, economy and the facility of large-area deposition. Thin film deposition of selenium rich chalcogenides has been reported by many researchers [6-9]

The structure of a-Se has two fold co-ordinations and it consists of long polymeric  $\text{Se}_n$  chains. In Se-Te alloys, Te enters in the structure by isoelectronic substitution. Addition of Te changes inter-chain bonding because the atomic size of Te is larger than that of Se. Se-Te alloys are quite useful due to their good performance in fields such as optoelectronics, integrated optics, optical imaging etc. over amorphous Se. Addition of Te in Se reduces the electronic band gap of Se to make it more useful [10]. Additive elements create compositionally and configurationally disordered system [11]. Thermal processes are of great significance in inducing crystallization in chalcogenide glasses. Separation of different crystalline phases with thermal annealing has been observed. Changes in optical properties have been found in thin films by heat treatment [12]. The effects of heat treatment, light-induced changes, ultraviolet irradiation etc. on the optical properties of chalcogenide thin films have been investigated by researchers [13, 14].

The present work investigates the effects of annealing on the structural, morphological and optical properties of cadmium and copper added selenium rich quaternary thin film  $\text{Se}_{50}\text{Cd}_{20}\text{Cu}_{20}\text{Te}_{10}$ .

## **2. EXPERIMENTAL DETAILS**

Bulk sample was prepared by melt quenching technique. 5N pure component materials purchased from Sigma Aldrich were weighed in proportion of their respective atomic weights. These were sealed in evacuated ( $10^{-3}$  Torr) quartz ampoules of length  $\sim 6$  cm and internal diameter  $\sim 8$  mm. The sealed ampoules were then heated in a furnace at a heating rate of  $4^\circ\text{C}/\text{min}$  upto  $1000^\circ\text{C}$  and were held at this temperature for 10 hours. After the stipulated duration, the obtained melt was cooled rapidly by dropping the ampoule into ice-cold water. The quenched sample was recovered which was then crushed to obtain bulk sample in the form of fine powder.

Thin film from the bulk sample was deposited on chemically cleaned glass substrates by thermal evaporation at a pressure  $\sim 4 \times 10^{-6}$  mbar using a molybdenum boat in HINDHIVAC coating unit Model No. 12A4D. During deposition, the temperature of the substrate was maintained at room temperature to avoid re-evaporation of any condensed component. Film of thickness 267 nm was synthesized. Post deposition, the films were annealed at the rate of  $5^\circ\text{C}/\text{min}$  from room temperature upto  $125^\circ\text{C}$  and

were kept at this temperature for two hours. These were then cooled gradually to room temperature.

The as-deposited and annealed films were characterized by X-ray Diffraction (XRD), Field Emission Scanning Electron Microscopy (FESEM), UV-Visible-NIR spectroscopy and Photoluminescence (PL) spectroscopy. XRD studies were done at a scanning rate of  $2^\circ/\text{min}$  employing  $\text{Cu K}\alpha$  radiation wavelength  $1.5404\text{\AA}$  by Ultima IV diffractometer from Rigaku, Japan. FESEM images were taken using JSM-7610F model from JEOL, Japan. Absorption and transmission spectra were recorded with the help of Jasco V670 UV-Vis-NIR spectrophotometer and Photoluminescence (PL) spectra were recorded using LS55 Perkin Elmer Fluorescence spectrometer. All the measurements were performed at room temperature.

### 3. RESULTS AND DISCUSSION

#### 3.1 X-ray Diffraction studies:

Figure 1 shows the X-ray diffraction patterns of the as-deposited and annealed  $\text{Se}_{50}\text{Cd}_{20}\text{Cu}_{20}\text{Te}_{10}$  films. It is clear that the as-deposited film has no sharp structural peaks and hence confirms its amorphous structure. On the other hand, when the film is annealed, crystallinity is introduced in amorphous phases and the film shows polycrystalline structure thereby indicating orientation of atoms along different planes [15-17].

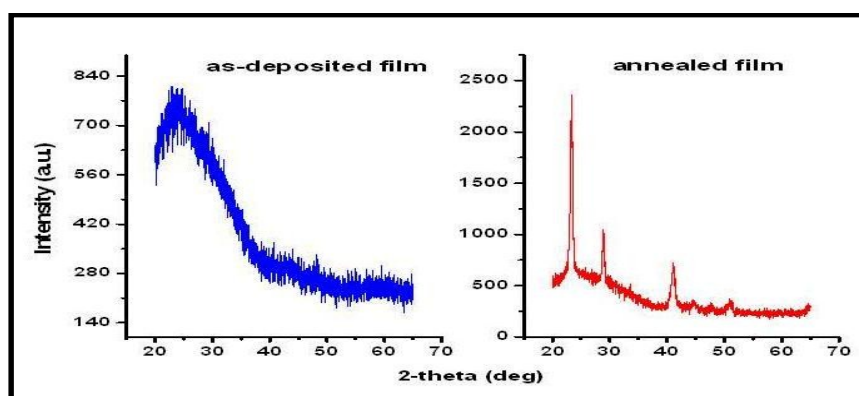
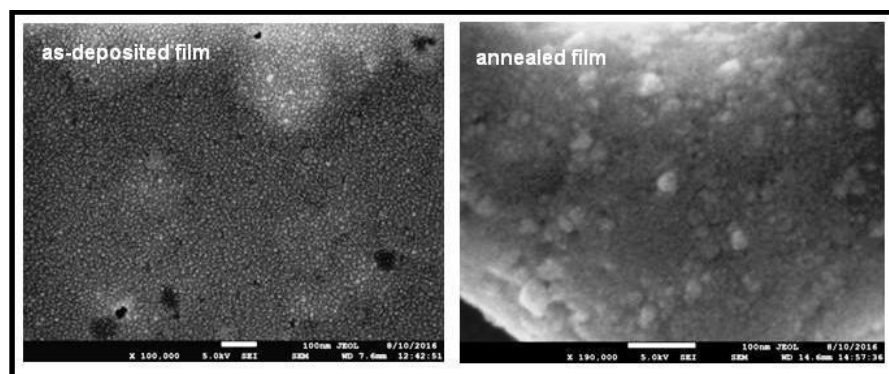


Figure 1. XRD patterns of as-deposited and annealed  $\text{Se}_{50}\text{Cd}_{20}\text{Cu}_{20}\text{Te}_{10}$  films

#### 3.2 Surface Morphological Studies:

Figure 2 shows the FESEM images of both the as-deposited and annealed  $\text{Se}_{50}\text{Cd}_{20}\text{Cu}_{20}\text{Te}_{10}$  films. Both the films reveal nano size of the grains. The as-deposited film shows uniformly scattered grains over the entire surface. The size of

the grains is  $\sim 10$  nm. When the film is subjected to heat treatment, the annealed film shows spongy nature. Again, it shows uniformly distributed grains but with increase in their size. The grains also show densification thereby reducing the grain boundary. In this case, the grains are  $\sim 15$ -20 nm. Such increase in the grain size due to post-deposition annealing has been reported by many researchers [18-20].



**Figure 2.** FESEM images of as-deposited and annealed  $\text{Se}_{50}\text{Cd}_{20}\text{Cu}_{20}\text{Te}_{10}$  films

### 3.3 Absorption Spectra:

Absorption spectra of the as-deposited and annealed films recorded in the near infrared (NIR) range 800 – 2700 nm are shown in Figure 3. Both the films have low absorption in this range. The annealed film shows slightly higher absorption as compared to the as-deposited film. This may be due to the morphological changes introduced due to annealing.

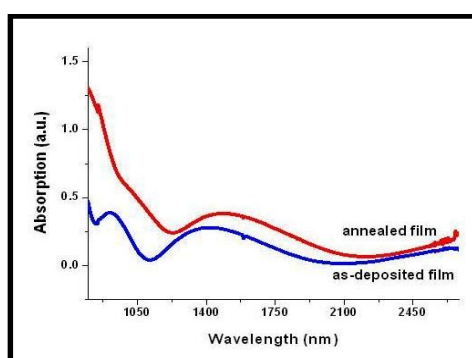


**Figure 3.** Absorption spectra of as-deposited and annealed  $\text{Se}_{50}\text{Cd}_{20}\text{Cu}_{20}\text{Te}_{10}$  films

### 3.4 Transmission spectra:

Figure 4 shows transmission spectra of both the as-deposited and annealed films in the spectral range 200 – 2700 nm. It is clear that both the films have zero or

insignificant transmission in the ultraviolet (UV) and visible regions.

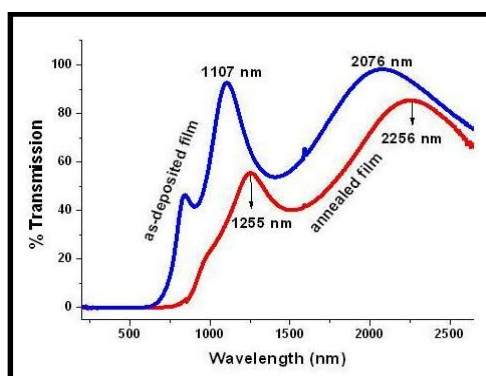


**Figure 4.** Transmission spectra of as-deposited and annealed  $\text{Se}_{50}\text{Cd}_{20}\text{Cu}_{20}\text{Te}_{10}$  films

In the NIR range, transmission gradually increases and interference maxima and minima are observed for both the films which indicate homogeneity of the films [21]. The curves show non-shrinking interference patterns which are indicative of thin good quality films. The as-deposited film shows transmission maxima of 93% and 99% at 1107 nm and 2076 nm respectively. Annealing reduces transmission substantially and maxima of only 56% and 86% are noticed at 1255 nm and 2256 nm respectively for the annealed film. Lower transmission of the annealed films can be attributed to structural changes and increased grain size as can be seen in the structural and morphological discussion. This is also reported by other researchers [22, 23]. The occurrence of spectral interference in these thin films may thus find utility in the desired infrared ranges.

### 3.5 Photoluminescence (PL) Spectroscopy:

Photoluminescence spectroscopy gives information with respect to the different energy states that are available between valence and conduction bands and are responsible for radiative recombination [24]. PL spectra have been recorded at three different excitation wavelengths ( $\lambda_{\text{ex}}$ ) – 330 nm, 380 nm and 430 nm – of UV and visible regions. Figure 5 shows PL spectra for as-deposited and annealed  $\text{Se}_{50}\text{Cd}_{20}\text{Cu}_{20}\text{Te}_{10}$  films at the three excitation wavelengths. It is seen that intense single emission bands are found in the green region at 527 nm (2.35 eV) and 513 nm (2.41 eV) for  $\lambda_{\text{ex}} = 330$  nm and 380 nm respectively whereas for  $\lambda_{\text{ex}} = 430$  nm, two green emission bands are found at 529 nm (2.34 eV) and 567 nm (2.18 eV). The films are, therefore, useful for optoelectronic applications.

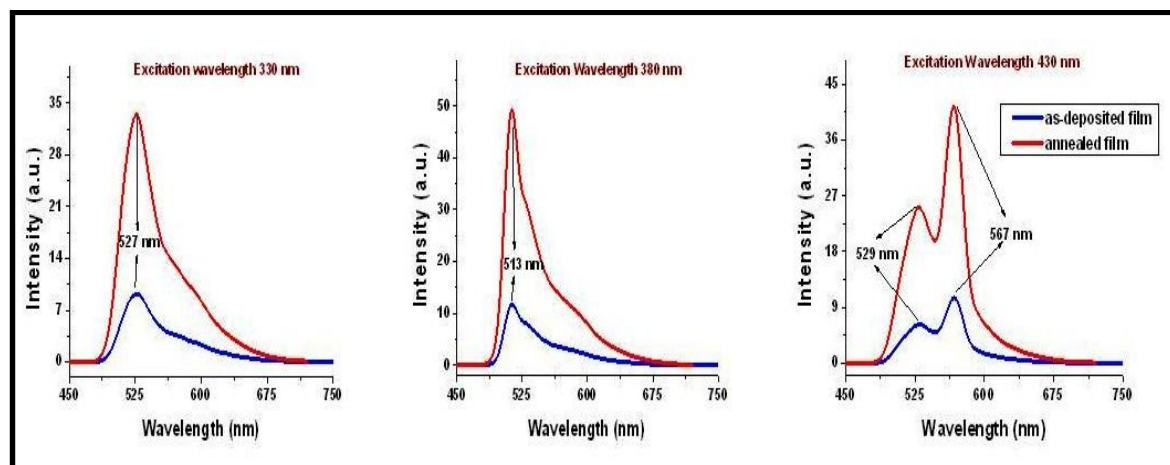


**Figure 5.** PL spectra at different excitation wavelengths for as-deposited and annealed  $\text{Se}_{50}\text{Cd}_{20}\text{Cu}_{20}\text{Te}_{10}$  films

Annealing does not at all change the emission wavelength for the three respective excitation wavelengths i.e. peak intensity of emission occurs at exactly the same wavelengths as for the as-deposited film. It is noticed that PL intensities show manifold increase due to annealing for all values of  $\lambda_{\text{ex}}$ . This may be due to modification of local electron distribution which increases the number of surface states involved in PL emission. Change in local electron distribution is quite likely to occur in view of changes observed in the structural and morphological analyses. With a view to compare performance of the as-deposited and annealed films with changing excitation wavelength, PL spectra are shown in Figure 6. It is observed that maximum PL emission occurs for  $\lambda_{\text{ex}} = 380$  nm in both the cases.

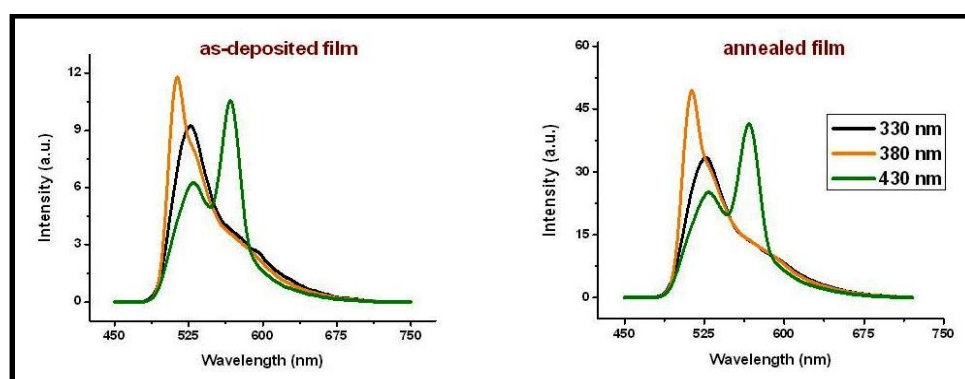


**Figure 6.** PL spectra of as-deposited and annealed  $\text{Se}_{50}\text{Cd}_{20}\text{Cu}_{20}\text{Te}_{10}$  films for the three excitation wavelengths

## CONCLUSIONS

Se<sub>50</sub>Cd<sub>20</sub>Cu<sub>20</sub>Te<sub>10</sub> thin film was deposited on glass substrate by thermal evaporation method. Bulk sample was synthesized using melt quenching technique. Post-deposition annealing was done at 125<sup>0</sup>C for two hours. Annealing improves the structural and morphological characteristics of the quaternary film in terms of giving it a more ordered and densified state. Absorption is low for both the films but transmission reaches upto 99 per cent at specific wavelength in the NIR region. Annealing reduces transmission but manifold increase in the PL intensity at same energy in green region signifies a more effective photoemission property. These properties make it a promising alternative for phase change memory media, IR optics and optoelectronic applications.

## ACKNOWLEDGEMENTS

Financial assistance from UGC, New Delhi vide project F. No. 42-773/2013(SR) is gratefully acknowledged. The authors express gratitude to Prof. Vinay Gupta, Department of Physics & Astrophysics, University of Delhi, India for providing facility to synthesize the thin film at his laboratory. Authors are also thankful to U.P. State Government through Centre of Excellence Scheme for providing XRD facility at the Department of Physics, University of Lucknow, Lucknow.

## REFERENCES

- [1] Massaccesi, S., Sanchez, S., and Vedel, J., 1993, "Cathodic Deposition of Copper Selenide Films on Tin Oxide in sulfate Solutions", *J. Electrochem. Soc.*, 140(9), pp. 2540-2546.
- [2] Ogah, O. E., Reddy, K. R., Zoppi, G., Forbes, I., and Miles, R. W., 2011, "Annealing studies and electrical properties of SnS based solar cells", *Thin Solid Films*, 519(21), pp. 7425-7428.
- [3] Nwofe, P. A., Ramakrishna Reddy, K. T., Sreedevi, G., Tan, J. K., and Miles, R. W., 2012, "Structural, Optical and Electro-optical Properties of Thermally Evaporate Tin Sulphide Layers", *Jpn. J. Appl. Phys.*, 51(10S), pp. 10NC36.
- [4] Agbo, P. E., and Nwofe, P. A., 2015, "Comprehensive studies on the optical properties of ZnO- Core shell thin films", *J. Nano. Adv. Mat.*, 3(2), pp. 63-67.
- [5] Chikwenze, R. A., Nwofe, P. A., Agbo, P. E., Nwankwo, S. N., Ekpe, J. E., and Nweke, F. U., 2015, "Effect of dip time on the structural and optical properties of chemically deposited CdSe thin films", *Int. J. Mater. Sci. Applic.*, 4(2), pp. 101-106.

- [6] Zimmer, J. P., Kim, S. W., Ohnishi, S., Tanaka, E., Frangioni, J. V., and Bawendi, M. G., 2006, "Size Series of Small Indium Arsenide-Zinc Selenide Core-shell Nanocrystals and their Applications to In Vivo Imaging", *J. Am. Chem. Soc.*, 128(8), pp. 2526-2527.
- [7] Di Giulio, M., Micocci, G., Rella, R., Siciliano, P., and Tepore, A., 1987, "Optical absorption and photoconductivity in amorphous indium selenide thin films", *Thin Solid Films*, 148(3), pp. 273-278.
- [8] Robinson, R. J., and Kun, Z. K., 1975, "p-n junction zinc sulfo-selenide and zinc selenide light-emitting diodes", *Appl. Phys. Lett.*, 27(2), pp. 74-76.
- [9] Garcia, V. M., Nair, P. K., and Nair, M. T. S., 1999, "Copper selenide thin films by chemical bath deposition", *J. Cryst. Growth*, 203(1), pp. 113-124.
- [10] Avrami, M., 1940, "Kinetics of Phase Change. II Transformation-Time Relations for Random Distribution of Nuclei", *J. Chem. Phys.*, 8, pp. 212-224.
- [11] Neetu, and Zulfeqar, M., 2013, "Annealing effect on optical parameters of  $\text{Se}_{85-x}\text{Te}_{15}\text{Hg}_x$  thin films", *J. Alloys Compd.*, 576, pp. 103-107.
- [12] Lafi Omar, A., and Imran Mousa, M. A., 2010, "The effect of gamma irradiation on glass transition temperature and thermal stability of  $\text{Se}_{96}\text{Sn}_4$  chalcogenide glass", *Radiat. Phys. Chem.*, 79(1), pp. 104-108.
- [13] Bahishti, A. A., Khan, M. A. M., Patel, B. S., Al-Hazmi, F. S. and Zulfeqar, M., 2009, "Effect of laser irradiation on thermal and optical properties of selenium-tellurium alloy", *J. Non-Cryst. Solids*, 355(45), pp. 2314-2317.
- [14] Marquez, E., Jimenez-Garay, R., and Gonzalez-Leal, J. M., 2009, "Light-induced changes in the structure and optical dispersion and absorption of amorphous  $\text{As}_{40}\text{S}_{20}\text{Se}_{40}$  thin films", *Mater. Chem. Phys.*, 115, pp. 751-756.
- [15] Yunxia, Z., Guanghai, L., Bo, Z., and Lide, Z., 2004, "Synthesis and characterization of hollow  $\text{Sb}_2\text{Se}_3$  nanospheres", *Materials Letters*, 58, pp. 2279-2282.
- [16] Yifeng, G., Zhitang, S., Ting, Z., Bo, L., and Songlin, F., 2010, "Novel phase-change material GeSbSe for application of three-level phase-change random access memory", *Solid-State Electronics*, 54, pp. 443-446.
- [17] Hafiz, M. M., El-Kabany, N., Kotb, H. M., and Bakier, Y. M., 2015, "Annealing Effects on Structural and Optical Properties of  $\text{Ge}_{10}\text{Sb}_{30}\text{Se}_{60}$  Thin Film", *Int. J. Thin. Fil. Sci. Tec.*, 4(3), pp. 163-171.
- [18] Nwofe, P. A., Miles, R. W., and Reddy, K. T. R., 2013, "Effects of sulphur and air annealing on the properties of thermally evaporated SnS layers for application in thin film solar cell devices", *J. Renew. Sustain. Energy*, 5(1),

pp. 011204.

- [19] Purohit, A., Chander, S., Nehra, S. P., Lal, C., and Dhaka, M. S., 2015, "Effect of thickness on structural, optical, electrical and morphological properties of nanocrystalline CdSe thin films for optoelectronic applications", *Opt. Mater.*, 47, pp. 345-353.
- [20] Chikwenze, R. A., Nwofe, P. A., Agbo, P. E., Famuyibo, D. A., Umahi, A. E., Ngele, S. O., and Ogah, S. P. I., 2015, "Annealing Effects and Film Thickness Dependence of Cobalt Selenide Thin Films Grown by the Chemical Bath Deposition Method", *IOSR Journal of Electronics and Communication Engineering*, 10(5), pp. 19-24.
- [21] Malik, K., Parvinder, Gupta, A., and Kumar, P., 2015, "Dispersive optical constants of thermally evaporated  $\text{Se}_{70-x}\text{Te}_{30}\text{Pb}_x$  thin films", *Journal of Ovonic Research*, 11(2), pp. 61-72.
- [22] Alterkop, B., Parkansky, N., Goldsmith, S., and Boxman, R. L., 2003, "Effect of air annealing on opto-electrical properties of amorphous tin oxide films", *J. Phys. D: Appl. Phys.*, 36(5), pp. 552-558.
- [23] Nair, M. T. S., Peña, Y., Campos, J., García, V. M., and Nair, P. K., 1998, "Chemically Deposited  $\text{Sb}_2\text{S}_3$  and  $\text{Sb}_2\text{S}_3$  - CuS Thin Films", *J. Electrochem. Soc.*, 145(6), pp. 2113-2120.
- [24] Nogriva, V., Dongre, J. K., Ramrakhiani, M., and Chandra, B. P., 2008, "Electro- and Photo-Luminescence Studies of CdS Nanocrystals prepared by organometallic precursor", *Chalcogenide Letters*, 5(12), pp. 365-373.

